IEEE Robotics and Automation Magazine (RAM) paper presented at
2024 IEEE/RSJ International Conference on Intelligent Robots and Systems (IROS)
October 14-18, 2024. Abu Dhabi, UAE

A Whole-Body Integrated AVATAR System: Implementation of Telepresence with Intuitive Control and Immersive Feedback

Sungman Park, Junsoo Kim, Hojae Lee, Minwoong Jo, Dohoon Gong , Dawon Ju, Dami Won, Sihyeon Kim, Jinhyeok Oh, Hun Jang, Joonbum Bae, Member, IEEE

***Abstract*—This paper proposes an intuitive and immersive whole-body teleoperation system with motion-based control and multi-modal feedback. The system consists of an anthropomorphic teleoperated robot and a haptic interface platform. The teleoperated robot has dual arms with dexterous hands, a head with a neck, a waist, giving it a human-like appearance and a large range of motion (ROM), as well as an omnidirectional mobile platform for improved mobility. The haptic interface platform enables a human operator to control the robot intuitively by measuring the operator's motion with a motion capture system, providing haptic feedback to the user's arms, fingers, and feet, and providing 3D image feedback. Additionally, facial animation further enhances immersion by synchronizing the face expression of the robot with the user's voice. The proposed teleoperation system offers a promising solution for the human-oriented robotic avatar system, which was verified through a global competition, the $10M ANA Avatar XPRIZE. The system was successfully evaluated with 45 minutes of training time for users who were new to our system. And the lessons learned from the competition and future improvements are discussed.**

***Index Terms*—Haptic, Teleoperation, Telepresence**

I. INTRODUCTION

Despite drastic advancements in artificial intelligence and automation technologies, robots are still incapable of surpassing human intelligence and adaptability to unexpected situations. Teleoperation technologies, which leverage human skills and judgment, are extensively used in disaster relief, including natural disasters and industrial accidents, as well as space and marine exploration. The COVID-19 pandemic has further highlighted the significance of teleoperation systems, not only in medical applications such as healthcare and rehabilitation but also in non-face-to-face and non-contact daily life. These systems have gained popularity across diverse domains, providing effective solutions for remote operations and thereby emerging as a vital element of the contemporary workforce.

To enhance the performance of teleoperated tasks, it is crucial to implement telepresence, which enables users to feel as if they are in the remote environment by intuitive and immersive system. One of the most effective ways to intuitively control a teleoperated robot is to mimic user motion and leverage humans' proprioception ability to perceive body position and movement without relying on visual or tactile senses [1]. To provide an immersive teleoperation experience, the teleoperation system should enable the robot to collect and communicate various forms of environmental information to the user, such as vision, audio, physical interaction, and distance, in an intuitive manner. This approach does not require extensive training, making it an efficient and user-friendly control mechanism, and provides the user with proprioception, which facilitates understanding of the robot's state [2, 3].

This paper introduces an advanced version of the interactive and intuitive control interface for a teleoperated robot (abbreviated AVATAR) system [4], including a tele-operated robot and a haptic interface platform for whole-body integrated telepresence as shown in Fig. 1. The teleoperated robot in the AVATAR system features two arms with 8 degrees of freedom (DOFs) and a waist with 2 DOFs. The robot's mobility is enabled by an omnidirectional mobile platform, while a triboelectric nanogenerator (TENG), force/torque, and ultrasonic sensors are used to measure various environmental information. The user interface has been upgraded to a haptic platform, comprising a haptic interface for imparting force feedback to the user's arm and hand, alongside a foot haptic controller for controlling the robot's mobile platform.

This work was supported by the National Research Foundation of Korea (NRF) Grant funded by the Korean Government (MSIT) (No.NRF-2019R1A2C2084677, 2022M3H4A1A02076825), and the Technology Innovation Program (20018112, Development of autonomous manipulation and gripping technology using imitation learning based on visual tactile sensing) funded by the Ministry of Trade, Industry & Energy (MOTIE, Korea).

Sungman Park, Junsoo Kim, Hojae Lee (equal contribution), Minwoong Jo, Dohoon Gong, Dawon Ju, Dami Won, Sihyeon Kim, Jinhyeok Oh, Hun Jang, and Joonbum Bae are with the Department of Mechanical Engineering, Ulsan National Institute of Science and Technology (UNIST), Ulsan, 44919, South Korea. (corresponding author to provide phone: +82-52-217-2335; e-mail: jbbae@unist.ac.kr) Now, Prof. Joonbum Bae is with the School of Mechanical Engineering, Korea University, Seoul, 02841, South Korea.

We participated in the $10M ANA Avatar XPRIZE competition with the name of Team UNIST, which aims to encourage the development of non-autonomous robotic technologies that enable remote operators to experience a sense of human presence in real-time, while performing various complex tasks suggested by the competition [5]. The AVATAR system was tested and evaluated during the semi-final and final rounds of competition, and its performance was assessed based on its ability to complete the designated tasks in a timely and efficient manner. Team UNIST achieved a rank of 6th among the 99 registered teams.

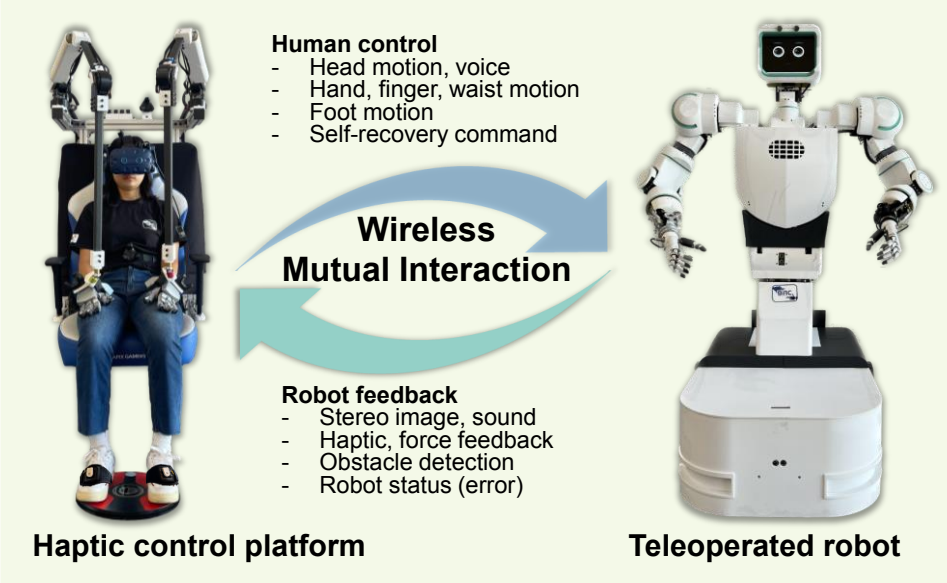

Fig. 1. Whole body integrated AVATAR system.

II. Related Work

The ultimate goal of teleoperation is to provide users with a sense of telepresence, enabling them to perceive and interact with the remote robot as if it were their own body. To achieve this, previous studies have investigated various approaches for communicating the user's intentions to a whole-body teleoperated robot, which includes not only manipulation but also mobility, while receiving information about the environment in an immersive way.

In previous research, grounded haptic devices and joysticks were used to control robots [6, 7]. However, these devices had limited DOFs and workspace, making it challenging for users to perform complex manipulations intuitively. Some researchers have utilized motion capture systems or even electromyography (EMG) sensors to enhance telepresence, synchronizing the robot's motions with the user's movements [8-10]. These interfaces have the advantage of being lightweight, small in volume, and not restricting the user's motions. However, teleoperation systems based on motion capture lack physical feedback and rely exclusively on visual feedback. This can lead to an increased cognitive workload for the user and limit the system's versatility in performing various tasks.

Therefore, researchers have explored haptic interface-based teleoperation systems, which provide physical feedback to the user's arm and hand while simultaneously measuring their motions. In [11–13], haptic interfaces were used to measure the user's movements, provide tactile feedback from the arm, and perform mobility control of the tele-operated robot using the user's leg or other arm not involved in the manipulation. In [14], an exo-suit that covers the entire body of the user was introduced to provide feedback to their arms and legs for interaction with the humanoid robot. This approach allows for intuitive control and appropriate physical feedback. However, the majority of teleoperated robots face limitations in their ability to perceive their environments, as they rely solely on three-dimensional images and measured forces from the robot's hands, arms, or legs, without considering the texture of the objects, surroundings, or the robot's status in the interaction.

III. Teleoperated Robot

A. Upper Body Design of the Teleoperated Robot

The teleoperated robot of the AVATAR system is designed to efficiently and effectively perform tasks with human-like structure and appearance as shown in Fig. 2. The upper body of the teleoperated robot is designed to mimic the skeletal structure of the human body. To ensure stable and accurate control of joint angles, the robot's upper body utilizes high-performance actuators with integrated controllers and encoders. The upper body kinematic structure includes 8 DOFs arms, 6 DOFs hands, a 2 DOFs waist, and a 3 DOFs neck as shown in Fig. 2. Anthropomorphic robotic arms are usually designed to have 7 DOFs, but the human shoulder complex should be considered for the natural motion generation, which has the additional translation and 3 DOFs rotations of the shoulder joint itself [15]. To achieve this, the upper body is designed with 8 DOFs (4 DOFs shoulder, 1 DOF elbow, and 3 DOFs wrist), allowing for a wider workspace and high manipulability. Additionally, robot manipulators generally have an offset between each actuator, which can cause a posture difference between the user and the robot, as the human wrist joint is spherical type. To solve this problem, we designed the wrist structure without offset by making the 7th joint axis intersect with the 8th joint axis through a 4-bar linkage, as shown in Fig. 3(a). The parallelogram mechanism simplifies the wrist structure and requires less maintenance than other transmission mechanisms, such as gears and chains.

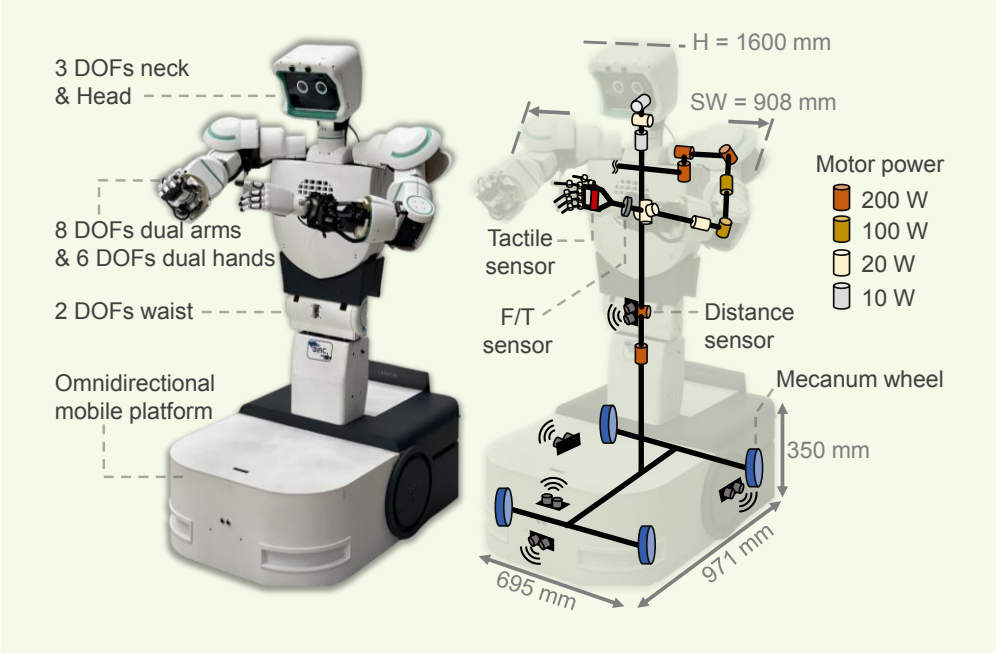

Fig. 2. Design and kinematic structure of the teleoperated robot. (H=height, SW=shoulder width)

The robot hands used in this system are 6 DOFs robot hands. Each finger, except for the thumb, has 1 DOF of flexion/extension. The thumb has 2 DOFs, consisting of flexion/extension and abduction/adduction. The robot's neck has 3 DOFs, and the robot's waist is designed with 2 DOFs (a yaw axis for horizontal movement and a pitch axis for leaning movement) by simplifying the human waist. Since the pitch axis needs to support the heavy robot upper body, a specially designed planetary gear with a reduction ratio of 3 and zero backlash was used to amplify the torque by 3 times as shown in Fig. 3(b). To remove backlash in the planetary gear for the waist pitch axis, anti-backlash gears were used in which two gears of the same shape are stacked at slightly different angles.

B. Kinematic Analysis for the Upper Body of the Teleoperated Robot

To enable intuitive control of the teleoperated robot and perform accurate task execution, it should closely follow the human's motions, while considering the robot's hardware limitations, such as joint angle limitations. To achieve this, we developed the inverse kinematics control algorithm shown in Fig. 4. The input to the algorithm includes the desired end-effector velocity and position, the arm posture angle, which is called as swivel angle [16], and the joint angle ranges of the robot, and the output is the joint angle that satisfies these conditions. However, numerical inverse kinematics can result in accumulated errors. So we addressed this issue by using closed loop inverse kinematics (CLIK), which compensates for errors in the task space [17].

To improve the stability of the robot arm near singularities and avoid joint limit violations, we implemented several methods. First, we used the damped least square (DLS) method, which adds a noise term λ to the pseudo-inverse. This method sacrifices some accuracy in inverse kinematics but improves the stability of the robot arm near singularities [18]. Additionally, we utilized the weighted least norm (WLN) method, which considers joint limit avoidance to keep the robot arm within the designated joint ranges [19]. The weighting matrix reduces joint movement as the joint approaches its limit. Finally, we incorporated the gradient projection method (GPM) as a redundancy control mechanism to match the arm posture angle of the human and robot. GPM adjusts the angle of the arm while maintaining the position of the robot hand by projecting the gradient of the performance criterion H into the null space of the Jacobian [20]. These methods work together to improve the robot's ability to perform tasks efficiently while staying within the designated joint ranges and avoiding singularities.

The final formula for the inverse kinematics algorithm is as follows:

$$\dot{q} = W^{-1}J^T(JW^{-1}J^T + \lambda^2 I)^{-1}(\dot{x_d} + Ke) + k_{arm}W^{-\frac{1}{2}}(I - J_w{}^{+}J_w)\nabla H \quad (1)$$

where $\dot{x_d}$ is the desired velocity of end-effector in the task space, J is Jacobian matrix of the robot arm, $\dot{q}$ is the joint velocity, λ is constant for DLS, K is a positive definite matrix which is tuned experimentally, e is the error between desired and present position of the robot hand, I is an identity matrix, W is a weighting matrix for avoidance of the joint angle limitation, $J_w = JW^{-\frac{1}{2}}$ represents the weighted Jacobian matrix, k_{arm} is a proportional gain of the GPM. The performance criterion H is a cost function, meaning the difference between the arm posture angles of the robot arm and the operator. The formula for H is as follows:

$$H = \frac{(\Psi_R - \Psi_O)^2}{2} \quad (3)$$

where Ψ_R and Ψ_O denote the arm posture angles of the robot arm and the operator, respectively.

C. Omnidirectional Mobile Platform

The omnidirectional mobile platform comprises four mecanum wheels, enabling the robot to move in any direction required to explore the environment and accomplish tasks. It includes a chassis and suspension system to distribute and supports the robot's weight, a base frame and enclosure to

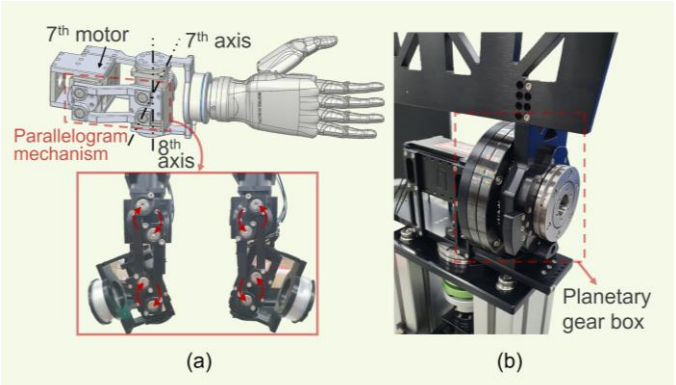

Fig. 3. Forearm and waist structure of the teleoperated robot. (a) Offset-free wrist structure and the robot hand. (b) Compact and zero backlash planetary gear.

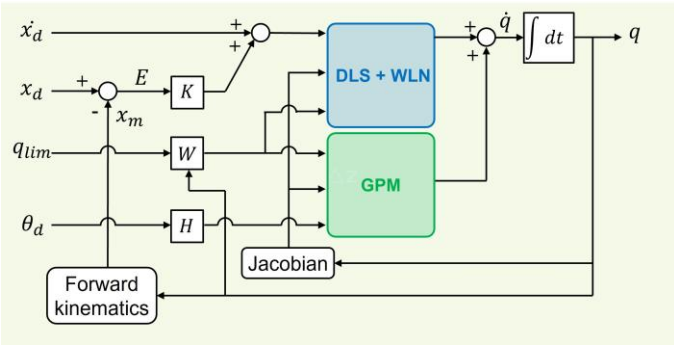

Fig. 4. Block diagram of the inverse kinematic algorithm of the teleoperated robot.

securely house necessary components such as a laptop, motor drivers, and batteries. To control the platform's speed, a trapezoidal speed profile is used, with the acceleration and deceleration slopes set differently based on experimental results. The maximum speed of the platform is 1.2 m/s, but the user-controlled speed is limited to 0.5 m/s to ensure safe robot movement and operation.

The omnidirectional mobile platform is equipped with five distance sensors are attached to the mobile platform: two on the front, one on each side, and one at the waist. The sensors on the sides are used to detect obstacles in the user's blind spot. The front two sensors measure the distance in the forward and upward directions, respectively. To guarantee safe operation on a work surface, such as a wall or desk, an algorithm has been implemented that automatically stops the mobile platform if the distance is less than a certain value.

D. Sensing System of the Teleoperated Robot

The robot is equipped with several sensors to provide immersive feedback to the user, including visual and auditory perception, force detection, texture determination, and distance sensing for mobility. A stereo camera with a lens spacing of 65 mm, equivalent to the average human pupil spacing, is attached to the robot's head to capture three-dimensional images. The stereo cameras offer 4416 x 1242

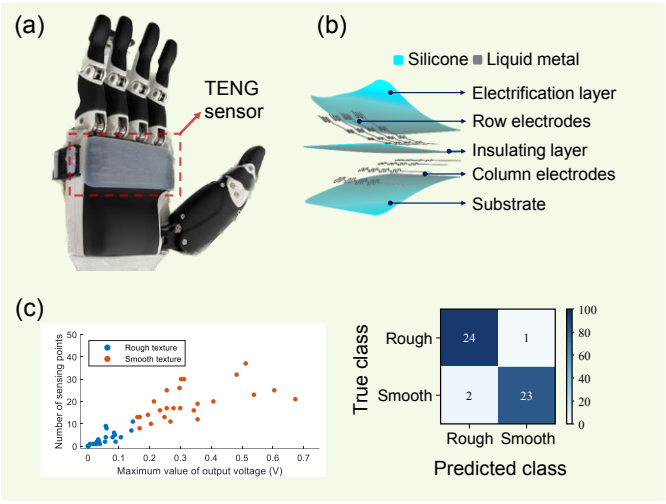

Fig. 5. Configuration of the TENG sensor and classification results. (a) Robot hand with TENG sensor (b) Graphic image of the structure of TENG sensor. (c) Data distribution of training sets for each texture and classification result.

(2.2 K) resolution image streaming at 30 Hz with a 90-degree horizontal field of view (FoV). The robot's body is equipped with speakers and microphones for auditory interaction, allowing the user's voice to be outputted and the environmental sounds to be transmitted to the user. A waist camera is attached to assist the user in manipulation when the view is obstructed by the movement of both arms. The waist view offers 720 x 480 (0.5 K) resolution image streaming at 30 Hz with a 78-degree horizontal FoV. 6 DOFs force torque (F/T) sensors, Robotous RFT64-SB01, are attached to the robot's wrist to measure the force generated through manipulation, with the maximum force and torque measurements of 200 N and 4.5 Nm, respectively. The fingers of the robot hand can measure the force through small load cells embedded in each finger. To ensure safe and stable operation, the error of the robot arm and finger from overload, as well as the measurement error of the F/T sensors and load cells, are measured to determine the robot status and delivered to the user.

To provide the robot with human-like surface texture sensing ability, we integrated a texture sensor into the robot's palm, as illustrated in Fig. 5(a). We developed a TENG sensor using liquid metal and silicone elastomers which have a simple structure, lightweight, self-powered operation, high stretchability, and electrical conductivity as shown in Fig. 5 (b). For real-time texture recognition, we designed the TENG sensor as a 4x4 array-shaped sheet. The support vector machine (SVM) algorithm was employed as a classification model, with the number of sensing points and maximum value of output voltage serving as input features. As shown in Fig. 5(c), a dataset consisting of 40 sets of sensing signals from four different subjects was used for training, and the texture recognition accuracy reached 94%.

IV. Haptic Control Platform

A. Haptic Interface

We have developed a haptic control platform, shown in Fig. 6(a), is used to track movements and provide immersive feedback to the user's entire body. A wearable haptic interface, shown in Fig. 6(b), provides force feedback on users' arms and fingers. This end-effector type interface has a simple structure and small volume, making it easy to use by users of different body sizes. It consists of 3 active DOFs and 3 passive DOFs, enabling translational force feedback in 3 DOFs. To reduce the load on the 2nd joint, which mainly receives its own weight, and to reduce physical fatigue caused by the interface's weight, we have applied a gravity compensation using a spring to the 2nd joint. Each link is designed to be 70 cm long to satisfy the user's arm's workspace while avoiding collisions. For 3 passive DOFs, a magnetic ball joint is applied to the end-effector, which allows the user to change the hand's orientation after wearing the interface without limiting wrist movement. The 3-axis force measured by the robot wrist is converted into the coordinate system of the user's end-effector, and the converted force is used to desired joint torque to control the 3 DOFs interface through kinematic analysis of the interface. Especially, when zero force is given as force feedback, complete back-drivability is guaranteed. The interface has a force capacity of up to 20 N and can be driven at up to 1 kHz. The haptic glove provides force feedback of up to 20 N to the user using a magnetic friction brake and vibration feedback using vibration motors embedded in the tips of the thumb and index finger and the back of the hand. The haptic glove and interface can be easily connected and disconnected by applying a spring-loaded bearing-lock mechanism.

The user's movements for controlling the robot are captured by a head-mounted display (HMD), the VIVE trackers, and the foot controller. An inertial sensor integrated into the HMD detects the user's head movements, while VIVE trackers attached to the haptic gloves and worn on the body track the upper body and arm motions. The process of measuring the user's movements involves calibrating the arms in a forward and outstretched position to ensure consistent robot control across different users. The haptic glove can measure four finger movements, excluding the ring finger. A specific gesture shown in Fig. 6(c) is chosen as a trigger for the robot's self-recovery algorithm, which automatically reboots the robot when an abnormality is detected in the arm, fingers, or F/T sensors. If the robot's abnormal status is conveyed to the user and the designated gesture is performed, the robot immediately reboots itself.

B. Visual and Auditory Feedback

The stereo camera mounted on the top of the robot's head captures the robot's environment to provide the user with stereoscopic three-dimensional video feedback. The two images from each lens of the stereo camera are merged into one image to reduce communication bandwidth, which is then transmitted from the robot to the user through the HMD. The received image is divided into two and displayed on the left and right displays of the HMD. Additional information measured by the sensing system of the robot is visually presented through the HMD as graphical elements on top of the stereo image, which include waist camera images, texture sensor information, distance information, and robot status information as shown in Fig. 7.

Auditory communication is also possible using a microphone and speaker located on the robot's chest and embedded in the HMD, respectively. On both the robot and user sides, analog voice signals sampled at 48 kHz. When the user speaks, the robot's face responds by blinking and changing the shape of its mouth for a more lifelike interaction, as illustrated in Fig. 8.

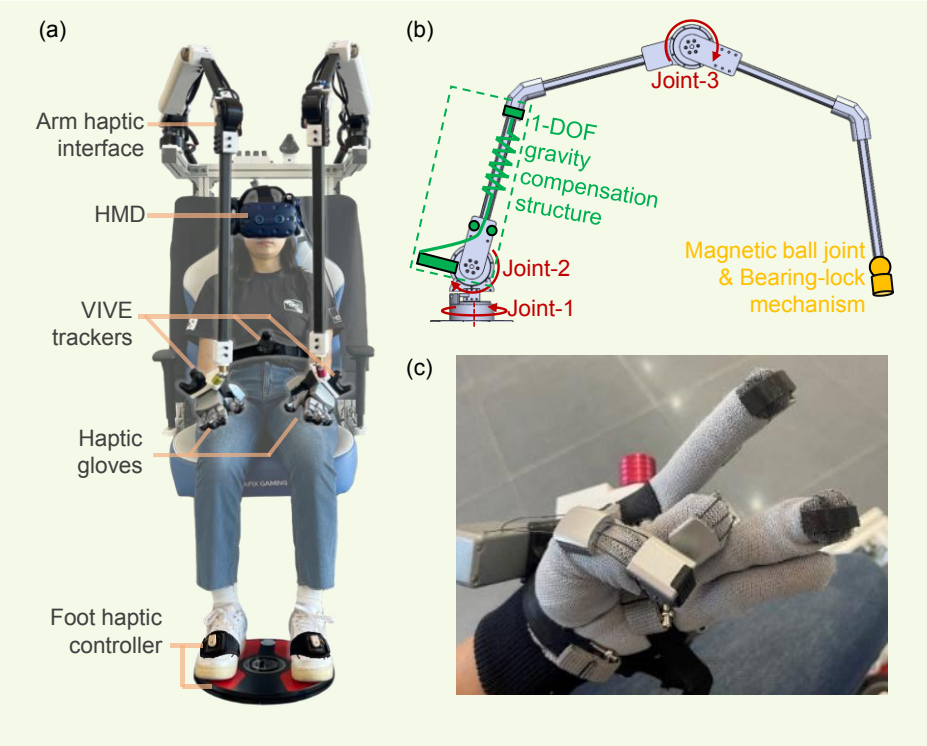

Fig. 6. Haptic control platform of the AVATAR system. (a) Haptic control platform. (b) Design of the arm haptic interface. (c) Haptic glove and trigger gesture for the self-recovery algorithm.

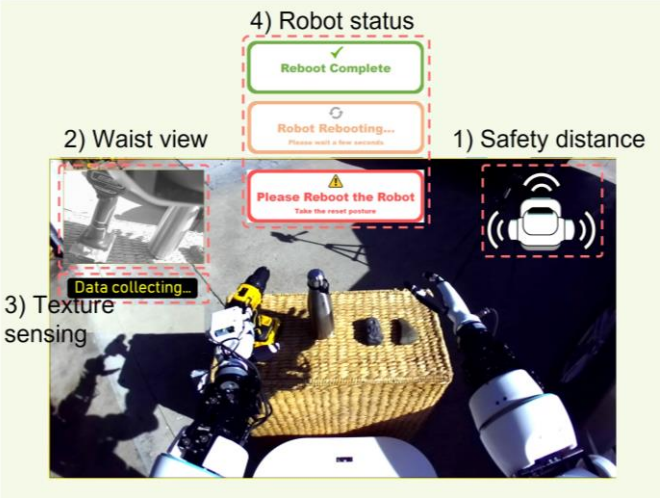

Fig. 7. Immersive 3D user′s view with various information of the teleoperation.

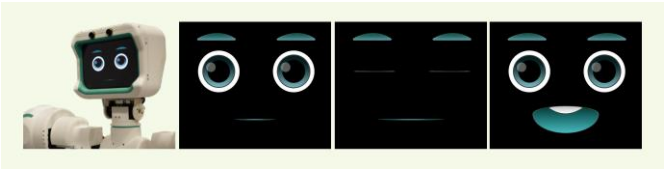

Fig. 8. Facial animation for the telepresence of the AVATAR system.

C. Foot Haptic Controller

We have incorporated a foot haptic controller by combining a commercially available 3D rudder with vibration feedback to enable omnidirectional control of a teleoperated robot. The 3D rudder serves as a motion controller, allowing manipulation through tilting forward/backward, left/right, and rotating counterclockwise/clockwise rotation. For the robot's safe navigation, the user wears a band equipped with an embedded vibration motor. This motor conveys information about the direction and proximity of surrounding obstacles, as detected by the robot's mobile platform, through patterns and intensities of vibration.

D. Communication of the System

The information measured by the robot and the haptic platform is delivered to the other party via user datagram protocol (UDP) communication for improved a real-time communication. To facilitate this communication, a bandwidth of up to 150 Mbps is required for each party. The stereo camera, with a resolution of 2.2 K, uses most of the bandwidth, and the bandwidth can be adjusted by changing the compression ratio of the image resolution based on the communication status. To account for communication delays and potential packet loss, the haptic control platform and teleoperated robot operate at 20 Hz each, as opposed to the 30 Hz image capture rate of the stereo camera.

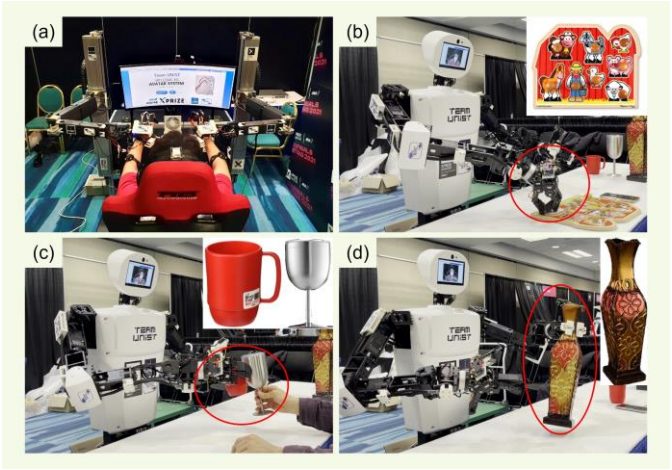

Fig. 9. Overview of the semi-final testing (a) Haptic control platform with an operator (b) Playing a collaborative puzzle. (c) Making a toast with a recipient. (d) Manipulating an artifact to describe the texture and the weight.

V. Performance Verification: $10M ANA Avatar XPRIZE

Our proposed teleoperation system was qualitatively evaluated during the semi-final and final testing of the $10M ANA Avatar XPRIZE [5]. In the semi-finals and finals, two judges from the competition evaluated how effectively the teleoperation system immersed them in the remote space and conveyed relevant sensory information, following the criteria outlined in the competition rules. (One was an operator who controlled the teleoperated robot in a separate room at least 100 meters away from the robot, and the other was a recipient on the robot side.) For every test, different judges who were unfamiliar to our system were assigned. In the semifinals and finals, we had to train them for 45 minutes, respectively.

A. Semi-final Testing of $10M ANA AVATAR XPRIZE

In the semi-finals, the evaluation was conducted in three scenarios (social interaction, business interaction, and cultural exchange) to test the capabilities of our previous version of the AVATAR system as shown in Fig. 9(a). Each scenario consisted of six tasks that included elements for evaluating the aforementioned capabilities. In the first scenario, the focus was on social interaction, and the objective was to collaboratively solve a peg puzzle with a recipient. In this scenario, the operator communicated with the recipient through the avatar robot with gestures and haptic feedback to correctly place the puzzles presented by the recipient, as shown in Fig. 9(b). The challenging point was to correctly place random sized puzzles. The second scenario focused on business interaction and involved performing verbal and physical interactions with the recipient, as shown in Fig. 9(c). Some mobility was required to get meeting to the table, where we chose one of the differently shaped cups to toast each other

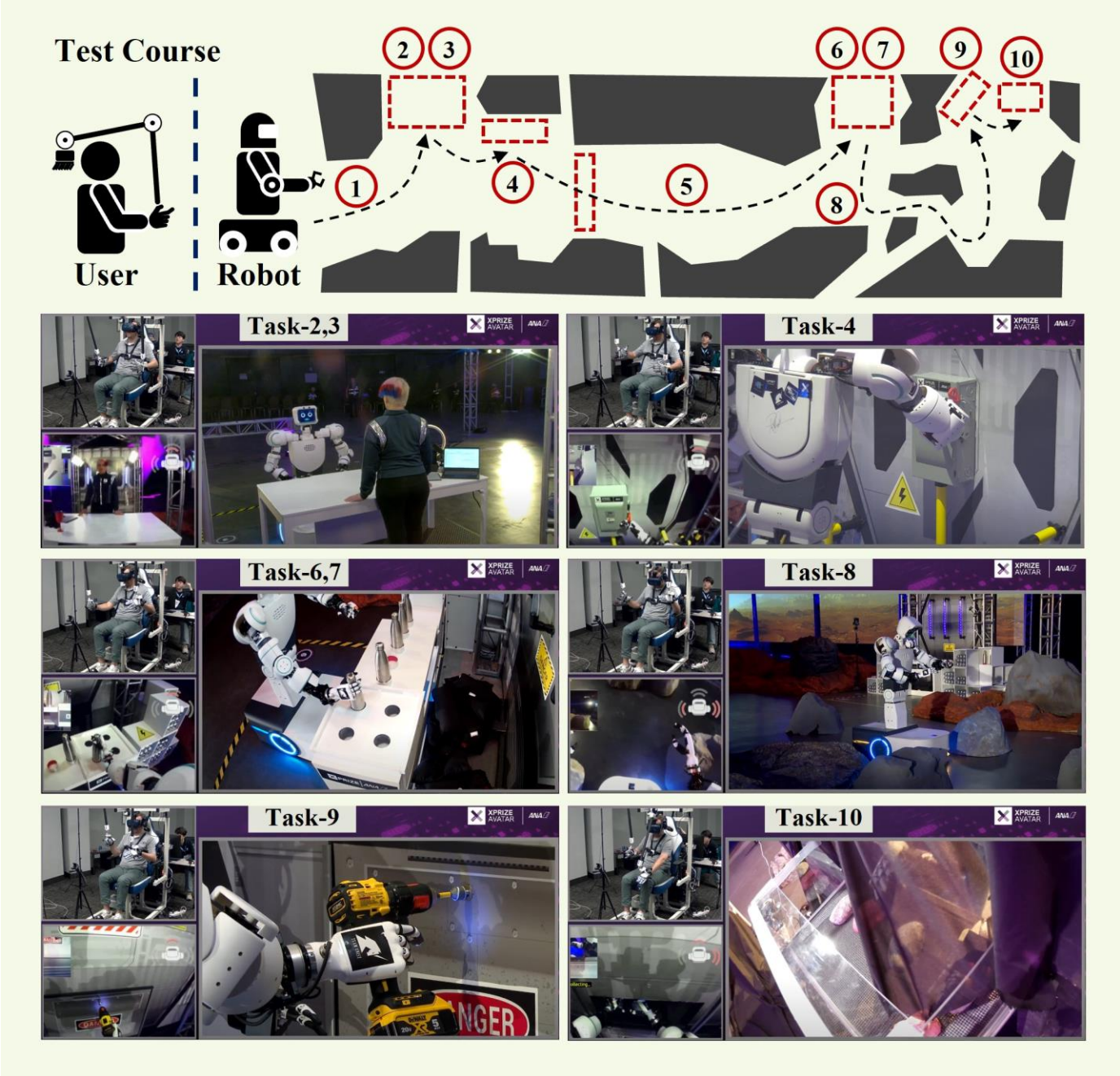

Fig. 10. The operator judge undergoing a final testing. (Top) Final testing course and 10 tasks of $10M ANA Avatar XPRIZE. (Task-2,3): Communicating with the mission commander. (Task 4): Activating a switch. (Task-6,7): Identifying the heavy canister (0.3 kg vs. 1.2 kg) and manipulating the heavy canister into the designated slot. (Task-8): Navigating through a narrow pathway. (Task-9): Utilizing a drill within the domain area. (Task-10): Feeling the texture of the object without seeing it and retrieving the requested one.

to celebrate a successful business deal. The last scenario was in the domain of cultural exchange and involved visiting a museum, experiencing an artifact, and explaining to the recipient what the operator felt. The challenging task was to feel and express the texture and weight of the artifact, as shown in Fig. 9(d). Using our system's vibration feedback for texture measurement based on soft sensors and force feedback through the haptic interface. As a result, we received a total score of 86 out of 100 points: 10 out of 10 points for the demonstration video submitted before the semi-finals, 33 out of 42 points for the operator judge, and 25 out of 30 points for the recipient judge, and 18 out of 18 points for the success of the scenario tasks. We ranked 15th out of 38 teams.

B. Final Testing of $10M ANA AVATAR XPRIZE

The final tasks was significantly more complex and challenging in comparison to those in the semi-final test. Unlike the semi-finals, the final was designed as a single scenario with three domains containing 10 tasks, all set on an unknown planet. The three domains were: Connection, which focused on facilitating immersive interactions between individuals despite distance; Exploration, which emphasized experiencing and navigating hazardous and unpredictable environments and Skill Transfer, involving the real-time delivery of essential skills and expertise to remote locations. Fig. 10 depict the final course and specific tasks.

Communication with the mission commander (Tasks 2 and 3) was facilitated through the robot's facial expressions and our system's visual and auditory feedback. For the navigating or moving tasks, we utilized an omnidirectional mobile platform and a foot haptic controller. In particular, when passing through a narrow pathway in Task 8, visual and foot haptic feedback through the distance sensing of the mobile platform was helpful. The system's intuitive control and haptic feedback were particularly useful in Tasks 4, 6, 7, and 9. In Task 9, the five-fingered robot hand allowed the user to operate the drill in the same way as the operator. In Task 10, a texture sensing system and back-of-the-hand haptic feedback based on classification results were utilized. Additionally, we activated the automatic stop algorithm in tasks involving walls or desks (Tasks 4, 6, 7, 9, and 10) to ensure the robot stopped in the correct position for manipulation. Although the robot briefly stopped during grasping the drill in Task 9 due to an overload error in the robot's fingers, it continued with the self-recovery algorithm, demonstrating the system's safety. As a result, we received a total score of 13.5 out of 15 points: 4.5 points for the operator and recipient judges, and 9 out of 10 points for the success of the scenario tasks (with a failure in 10th task within the given time). We ranked 6th out of 17 teams. We were the team that had the second-highest increase in rank based on the semi-final results. For more details, see [5].

C. Lessons Learned

Upon reflecting on our experience in the semi-finals and finals of the competition, we were reminded of the critical components required for successful teleoperation and the reliably integrated system that made these elements possible.

First of all, replicating the complexity of the human hand entirely is challenging, even if our goal is to construct the robot that mirrors the user's actions for intuitive control. As a result, in the final Task 10, the robot encountered challenges in recognizing and manipulating an invisible object based solely on texture and tactile feedback. We discovered that the robot's design and control still require improvement to accurately mimic human natural movement.

Secondly, the control interface should be simple to use and user-friendly. Even though we satisfied the demands of the range and speed of user arm motions with the haptic interface discussed in Section 4, and ensured easy removal of the haptic interface after wearing the haptic glove, some judges pointed out the inconvenience of wearing and operating the foot controller. They also faced difficulty in wearing the HMD after wearing all the interfaces. Future development should prioritize the easy wearability of the whole-body wearable haptic. Also, we recognized that visual information should be effectively provided to the user for safe and seamless operation. Our AVATAR system visually displayed an extensive amount of information to users via the HMD, including the main stereo camera and the single waist camera, the presence and distance of obstacles surrounding the mobile platform, texture classification results, and robot status. Therefore, it could have been difficult for users to understand all of the information. In fact, some judges had difficulty interpreting all of the information provided by the visual feedback.

Finally, achieving seamless teleoperation requires careful consideration of network issues. We adjusted the driving bandwidth and the update time of the communication loop based on the sampling frequency of the stereo camera to synchronize with the user's motions and feedback. This ensures a constant delay under a certain delay time and helps the user adapt easily. However, we encountered a serious problem when an unexpected drop in communication bandwidth occurred. Therefore, it is important to develop a guaranteed backup plan to address network issues in the future.

VI. Conclusion

This paper presents a whole-body integrated teleoperation system that allows for intuitive and immersive control by providing telepresence through motion-based control and visual, auditory, and haptic feedback. The haptic control platform and teleoperated robot were integrated with the UDP network with experimentally optimized bandwidth for real-time teleoperation. The AVATAR system was evaluated in the $10M ANA Avatar XPRIZE, where it was tested by judges who were new to the system. As a result, the proposed AVATAR system placed 6th out of 17 finalists. The qualitative evaluation indicates that the AVATAR system is effective and has the potential to be an innovative solution for teleoperated robot control.

References

[1] N. Colella, M. Bianchi, G. Grioli, A. Bicchi and M. G. Catalano, "A Novel Skin-Stretch Haptic Device for Intuitive Control of Robotic Prostheses and Avatars," *IEEE Robotics and Automation Letters*, vol. 4, no. 2, pp. 1572-1579, 2019.

[2] D. Hagner and J. G. Webstero, "Telepresence for touch and proprioception in teleoperator systems," *IEEE Transactions on Systems, Man, and Cybernetics*, vol. 18, no. 6, pp. 1020–1023, 1988.

[3] J. I. Lipton, A. J. Fay, and D. Rus, "Baxter's homunculus: virtual reality spaces for teleoperation in manufacturing," *IEEE Robotics and Automation Letters*, vol. 3, no. 1, pp. 179–186, 2018.

[4] S. Park, Y. Jung, and J. BAE, "An interactive and intuitive control interface for a tele-operated robot (AVATAR) system," *Mechatronics*, Vol. 55, pp. 54-62, 2018.

[5] XPRIZE, “Anywhere is possible.” Accessed on: March, 2023. [Online]. Available: https://avatar.xprize.org/.
[6] D. Ryu, J. Song, C. Cho, S. Kang and M. Kim, “Development of a six DOF haptic master for teleoperation of a mobile manipulator,” *Mechatronics*, Vol. 20, pp. 181-191, 2010.
[7] K. D. Katyal, C. Y. Brown, S. A. Hechtman, M. P. Para, T. G. McGee, K. C. Wolfe, R. J. Murphy, M. D.M. Kutzer, E. W. Tunstel, M. P. McLoughlin, and M. S. Johannes, "Approaches to robotic teleoperation in a disaster scenario: From supervised autonomy to direct control," *IEEE/RSJ International Conference on Intelligent Robots and Systems (IROS)*, pp. 1874-1881, 2014.
[8] L. Penco, N. Scianca, V. Modugno, L. Lanari, G. Oriolo and S. Ivaldi, "A multimode teleoperation framework for humanoid loco-manipulation: an application for the iCub robot," *IEEE Robotics & Automation Magazine*, vol. 26, no. 4, pp. 73-82, 2019.
[9] Y. Wu, P. Balatti, M. Lorenzini, F. Zhao, W. Kim and A. Ajoudani, "A teleoperation interface for loco-manipulation control of mobile collaborative robotic assistant," *IEEE Robotics and Automation Letters*, vol. 4, no. 4, pp. 3593-3600, 2019.
[10] G. Lentini, A. Settimi, D. Caporale, M. Garabini, G. Grioli, L. Pallottino, M. G. Catalano, and A. Bicchi, "Alter-ego: a mobile robot with a functionally anthropomorphic upper body designed for physical interaction," *IEEE Robotics & Automation Magazine*, vol. 26, no. 4, pp. 94-107, 2019.
[11] F. Abi-Farrajl, B. Henze, A. Werner, M. Panzirsch, C. Ott and M. A. Roa, "Humanoid teleoperation using task-relevant haptic feedback," *IEEE/RSJ International Conference on Intelligent Robots and Systems (IROS)*, pp. 5010-5017, 2018.
[12] C. Zhou, L. Zhao, H. Wang, L. Chen and Y. Zheng, "A bilateral dual-arm teleoperation robot system with a unified control architecture," *2021 30th IEEE International Conference on Robot & Human Interactive Communication (RO-MAN)*, pp. 495-502, 2021.
[13] R. Luo, C. Wang, E. Schwarm, C. Keil, E. Mendoza, P. Kaveti, S. Alt, H. Singh, T. Padır and J. P. Whitney, "Towards Robot Avatars: Systems and Methods for Teleinteraction at Avatar XPRIZE Semi-Finals," *IEEE/RSJ International Conference on Intelligent Robots and Systems (IROS)*, pp. 7726-7733, 2022.
[14] Y. Ishiguro, T. Makabe, Y. Nagamatsu, Y. K. Kojima , F. Sugai, Y. Kakiuchi, K. Okada, and M. Inaba, "Bilateral humanoid teleoperation system using whole-body exoskeleton cockpit TABLIS," *IEEE Robotics and Automation Letters*, vol. 5, no. 4, pp. 6419-6426, 2020.
[15] D. Lee, H. Park, J. Park, M. Baeg, and J. Bae, "Design of an anthropomorphic dual-arm robot with biologically inspired 8-DOF arms," *Intelligent Service Robotics*, vol. 10, no. 2, pp. 137-148, 2017.
[16] H. Kim, L. M. Miller, N. Byl, G. M. Abrams, J. Rosen, “Redundancy resolution of the human arm and an upper limb exoskeleton,” *IEEE transactions on biomedical engineering,* vol. 59, no. 6, pp. 1770-1779, 2012
[17] J. Wang, Y. Li, X. Zhao, “Inverse Kinematics and Control of a 7-DOF Redundant Manipulator Based on the Closed-Loop Algorithm,” *International Journal of Advanced Robotic Systems,* vol. 7, no. 4, pp. 37, 2010.
[18] S. Chiaverini, B. Siciliano and O. Egeland, "Review of the damped least-squares inverse kinematics with experiments on an industrial robot manipulator," *IEEE Transactions on Control Systems Technology*, vol. 2, no. 2, pp. 123-134, 1994.
[19] T. F. Chan and R. V. Dubey, "A weighted least-norm solution based scheme for avoiding joint limits for redundant joint manipulators," *IEEE Transactions on Robotics and Automation*, vol. 11, no. 2, pp. 286-292, 1995.
[20] H. Su, W. Qi, Y. Hu, H. R. Karimi, G. Ferrigno and E. D. Momi, "An Incremental Learning Framework for Human-Like Redundancy Optimization of Anthropomorphic Manipulators," *IEEE Transactions on Industrial Informatics*, vol. 18, no. 3, pp. 1864-1872, 2022.